IOSR Journal Of Pharmacywww.iosrphr.org
(e)-ISSN: 2250-3013, (p)-ISSN: 2319-4219
PP. 43-48

A Comparative Study on the Electrical And Thermal Properties of The Chemically Synthesized Copolymer, Poly(2-Methoxyaniline-Co-2-Chloroaniline) And Its Nanocomposite, Poly(2-Methoxyaniline-Co-2-Chloroaniline) –Composite- Fe_2O_3

P.Lakshmi[1,] S.JhancyMary[2]
[1]*Research Scholar,Department of Chemistry, Auxilium College, Vellore, Tamilnadu, India*
[2]*Asso.Prof. of Chemistry, Department of Chemistry, Auxilium College, Vellore, Tamilnadu, India*
[2]*Corresponding Author: Tel: 0416-2244130; Email address: jhancy2011@gmail.com*

ABSTRACT: *The copolymer of 2-chloro aniline and 2-methoxy aniline and its nano composite with iron oxide nanoparticles, Fe_2O_3 were synthesized by chemical oxidative polymerization technique using ammonium persulphate as the oxidizing agent and HCl and sodium lauryl sulphate as dopants. The materials synthesized were soluble in common organic solvents such as CCl_4, DMSO, alcohol and DMF. The presence of the anionic surfactant as the dopant improved the processability and the solubility of the materials. FTIR spectroscopy, UV-Visible spectroscopy, TGA and XRD studies confirmed the formation of the composite. The composite is thermally more stable than the copolymer. The electrical conductivities measured are in the semiconducting range and the composite showed greater electrical conductivity than the pure copolymer.*

Keywords: *conducting polymer, iron oxide nanoparticles, oxidative polymerization, poly (2-methoxy aniline-co-2-chloro aniline, semiconducting.*

I. INTRODUCTION

Conducting polymer inorganic nanocomposites attracted both fundamental and practical interest because of their different chemical, biological and physical properties and application in high density magnetic recording, catalysis, magnetic resonance imaging, energy conversion etc [1-4]. Among all the conducting polymers, polyaniline is one of the most promising conducting polymers due to its ease of preparation, good environmental stability, better electronic properties, low cost, low density and its applications in electrochromic display, electro catalysis, rechargeable batteries, sensors and biosensors [5-14]. Substituted polyanilines and copolymers of substituted polyanilines are also widely studied in the recent past due to improved properties and unique applications in electronics. Polymer nanocomposites are also known as nanostructured materials because it improves the performance properties of the polymer by doping inorganic nanoparticles [15]. Among all the metal oxide nanoparticles, iron oxides have attracted technological importance and potential applications in catalysis such as magnetic storage devices, ferrofluids and other uses [16]. In the present work, the synthesis and characterization of the copolymer, poly(2- methoxy aniline–co- 2 - chloro aniline) and its nanocomposite, poly(2 - methoxy aniline-co- 2- chloro aniline)/Fe_2O_3 nanocomposite in the presence of HCl and sodium lauryl sulphate as dopants and $(NH_4)_2S_2O_8$ as oxidant at 0℃ are reported. There are no reports on the composites of copolymers to the best of our knowledge.

II. EXPERIMENTAL

2.1 Chemical synthesis of the copolymer composite(poly(OMA-co-OCA/Fe_2O_3) and the copolymer(poly (OMA-CO-OCA)/SDS)

2-chloroaniline (6.4ml, 0.1mol), 2-methoxy aniline (6.2ml, 0.1mol), SDS (1.44 g in 50ml, 0.1 M) and 0.63g Fe_2O_3 (5%) were stirred in the reaction vessel maintained in the freezing mixture bath to obtain a homogeneous suspension. HCl (1M, 100ml) and ammonium persulphate (22.8g, 0.2mol in 100ml) were added dropwise with constant stirring over a period of four hours. The stirring was continued for two hours. It was kept at 0°C overnight, filtered, washed with deionized water and finally with few drops of acetone to remove the oligomers. The composite was then a suspended in deionized water and stirred for an hour on a magnetic stirrer and filtered. The washing of the product was continued till the filtrate was free of acid, dried in air and powdered. The % yield of the product is 33.3 %. The composite is soluble in CCl_4, DMSO, Alcohol and DMF. The pure copolymer, poly (OMA-CO-OCA)/SDS was also synthesized by oxidative polymerization technique for comparison of the thermal and electrical properties.

2.2 Characterization Techniques

The FT-IR spectra were recorded on a thermo Nicolet Avatar 370 spectrophotometer. The UV visible absorption spectra of the samples in DMSO were recorded using Perkin Elmer Lambda 35 spectrophotometer. The thermogravimetric analysis (TGA-DTA) was carried out in a SDT Q600 V20.9 built under inert gas atmosphere using a constant heating rate of 0℃ to 800℃ at 10 ℃/min. The X-ray diffraction patterns were recorded for the powdered materials with a Bruker AXS D8 Advance X-ray diffractometer using Cu- Kα of wave length 1.5406A°.

2.3. Electrical conductivity measurements

The electrochemical measurements were performed on a CHI608E electrochemical workstation in a conventional three electrode configuration with a Pt wire as counter electrode, Ag/AgCl in 1M KCl as a reference electrode and the synthesized copolymer material as working electrode. A 1M H_2SO_4 aqueous solution was prepared by doctor blade method using scotch tape as spacer. In the typical preparation, 5mg of the synthesized copolymer material was ground with 10µL of Triton X-100 and 20µL of deionized water to make a slurry. The slurry was spread on a 1.5x1.5 cm^2 fluorine- doped tin oxide (FTO) glass substrate with an active area about 0.5 cm^2 and then dried in hot plate at 80°C for 3 hours .

III. RESULTS AND DISCUSSION

3.1 Fourier Transform Infrared spectroscopy studies

The IR spectra of poly (OMA-CO-OCA)/SDS and poly(OMA-co-OCA/Fe_2O_3 are given in Fig.1 and Fig. 2. and the IR characteristic frequencies are tabulated in Table 1.

The IR spectrum of poly(OMA-co-OCA/Fe_2O_3 shows the peak around 3193 cm^{-1} due to N-H stretching. The peak around 1581 cm^{-1} is due to quinonoid rings (N=Q=N) and the peak around 1501 cm^{-1} is due to benzenoid rings (N-B-N). The peak around 1293 cm^{-1} is due to C-N stretching vibration. The peak around 747 cm^{-1} in the in the composite indicates the presence of C-Cl group. The peak at 1018 cm^{-1} is assigned to the symmetrical stretching of C-O-C bonds due to the presence of O-CH_3 group in the copolymer . The bands around 2926 cm^{-1} and 2845 cm^{-1} are due to the asymmetric and symmetric stretching vibration of C-H bond. The C-H out of plane bending vibration of the 1,2,4 tri substituted benzene rings appear at 834 cm^{-1}. The Fe-O linkage is shown around 542cm^{-1} in the copolymer composite. The IR spectrum shows the presence of all the characteristic bands and hence it was confirmed that the composite has been formed. It is well known that in systems with polyanilines,strong guest-host interaction such as hydrogen bonding occur in the form of NH-----O-H and -N-H----O-Fe in the composite respectively [17]. The weak intermolecular hydrogen bonding holds the chains together. By comparing the IR spectra of copolymer and copolymer/iron oxide nanocomposite, it is observed that in the composite the characteristic stretching frequencies are shifted towards lower frequencies due to weak Vander walls forces of attraction between iron oxide and copolymer chains.

Table 1: IR characteristic frequencies of (poly OMA-CO-OCA)/SDS and poly(OMA-co-OCA/ Fe_2O_3 nano composite

Peak Assignment	**Poly(OMA-co-OCA) /SDS** **cm^{-1}**	**Poly(OMA-co-OCA)/ Fe_2O_3** **cm^{-1}**
-NH stretching	3291	3193
-C=C- stretching of Quinonoid	1585	1581
-C=C- stretching of Benzenoid	1508	1501
C-H asymmetric & symmetric stretching	2930 & 2850	2926 & 2845
1,2,4 trisubstituted benzene	840	834
C-Cl stretching	747	747
C-H stretching of OCH_3	1028	1018
C-N stretching	1294	1293
Fe_2O_3 stretching in the composite	---	542

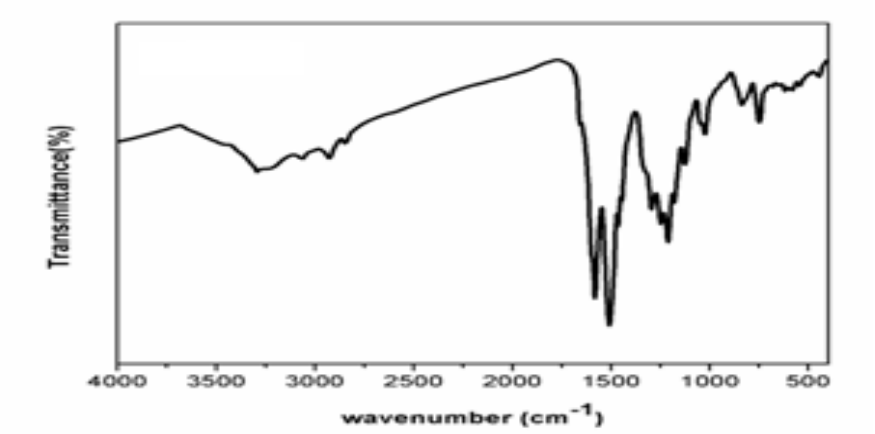

Figure 1: FT-IR spectrum of poly(OMA-co-OCA/ SDS

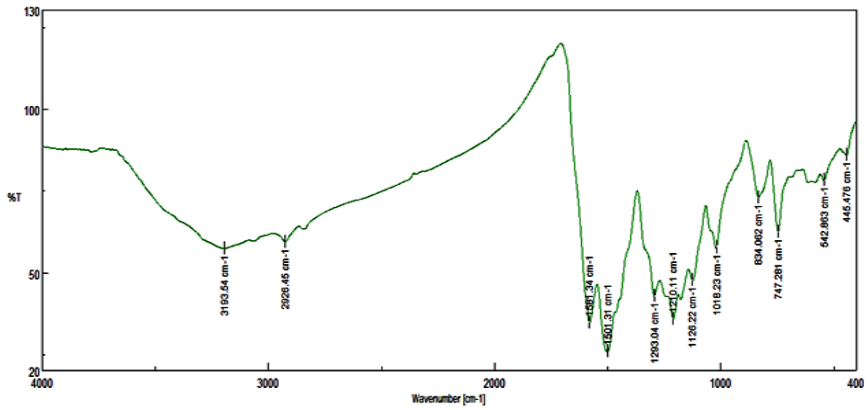

Figure 2: FT-IR spectrum of poly(OMA-co-OCA/ Fe_2O_3 nano composite.

3.2. UV Visible spectra

The UV –Visible spectra of poly (OMA-co-OCA/ Fe_20_3 nano composite is shown in Fig 3. The absorption around 275 nm represents the π-π* transition and the absorption around 405 nm is due to n-π* transition. The band around 575 nm is due to quinonoid ring transition between transfer from the highest occupied molecular orbital of the benzenoid ring to the lowest unoccupied molecular orbital of the quinonoid ring.

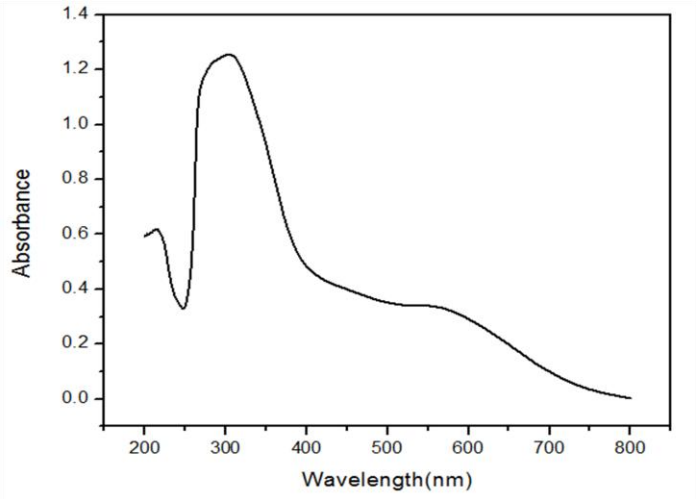

Figure 3: UV –Vis spectrum of poly(OMA-co-OCA/ Fe_2O_3 nano composite

3.3. TGA/DSC Analysis

The copolymer synthesized shows the loss of HCl around 220℃ and the degradation of the polymer takes place around 248℃ itself as shown in Fig. 4. The TGA and DSC of poly(OMA-co-OCA/ Fe_2O_3 composite are shown in Fig. 5. The composite undergoes weight loss in three steps. The weight loss around 100°C is due to the loss of volatile impurities and moisture. The loss of the dopants take place at 300℃ and the decomposition of the copolymer composite take place around 400℃ as shown in the figure. The DSC shows a broad exothermic melting at 379°C. The nanocomposite has greater thermal stability than the copolymer.

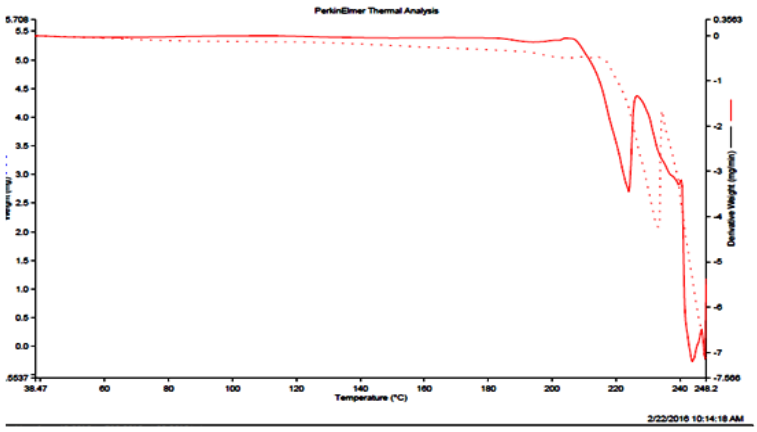

Figure 4: TGA of poly(OMA-co-OCA/SDS

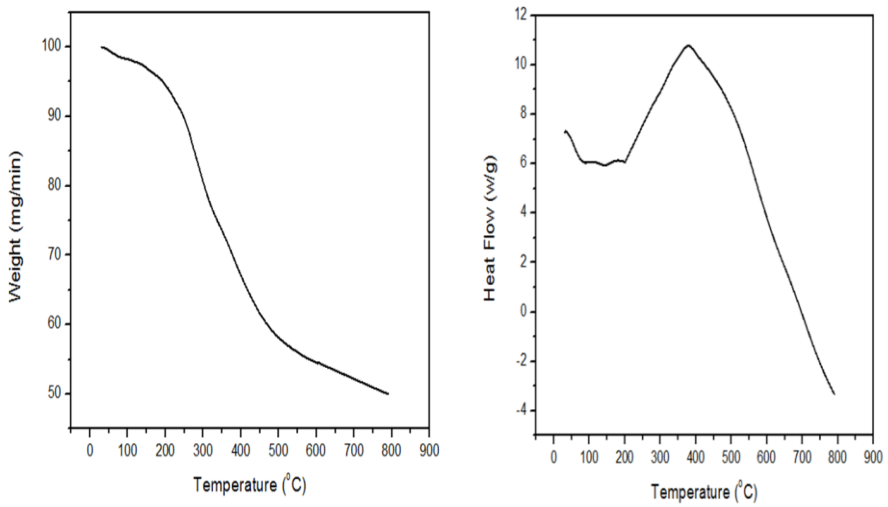

Figure: 5 TGA and DSC of poly(OMA-co-OCA/ Fe_2O_3 nano composite

3.4. X-Ray diffraction studies

The XRD pattern of poly (OMA-co-OCA) / Fe_2O_3 is shown in Fig. 6. The diffraction peaks of poly (OMA-co-OCA /Fe_2O_3 synthesized in the presence of SDS shows peaks around 2θ= 26°, 32° indicating that the composite is partially crystalline in nature. From the XRD data, the average crystalline size has been calculated by using Debye Scherrer equation:

$$D=0.89\ \lambda\ /\beta\cos\theta$$

where λ is the wave length of X ray, β is FWHM(full width at half maximum) , θ is Bragg angle and D is average particle size. The crystalline sizes of the (OMA-co-OCA) / Fe_2O_3 composite is calculated and given in Table 2.

Table 2: Average particle sizes calculated from XRD pattern

S.No.	Wave length □ (nm)	FWHM □	Angle	Average particle size D
1	0.154	0.00250	12.259	56.12
2	0.154	0.001	13.394	14.08

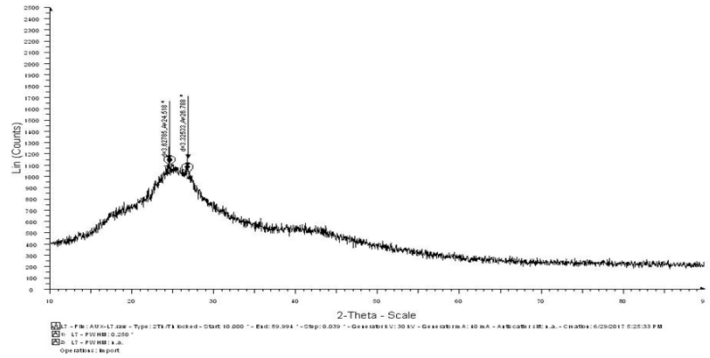

Figure 6: XRD Pattern of poly(OMA-co-OCA/ Fe_2O_3 nano composite.

3.5. Electrical Conductivity studies

The impedance plots of (poly OMA-CO-OCA)/SDS and poly(OMA-co-OCA/ Fe_2O_3 nano composite are shown in Fig.7 and Fig 8 respectively and the electrical conductivities are tabulated in Table 3.

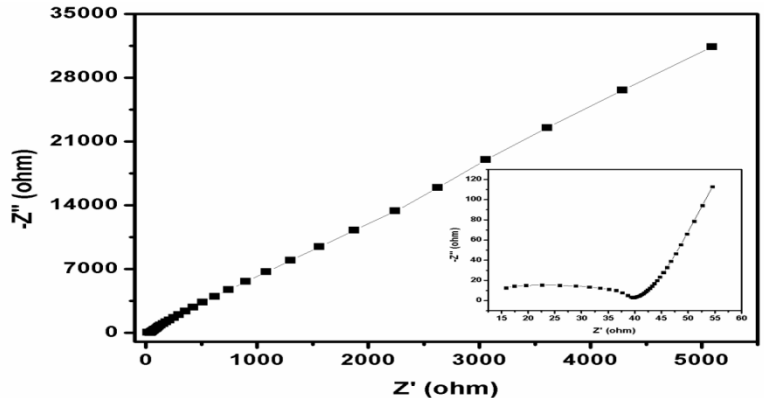

Figure7: Impedance plot of poly(OMA-co-OCA)/SDS

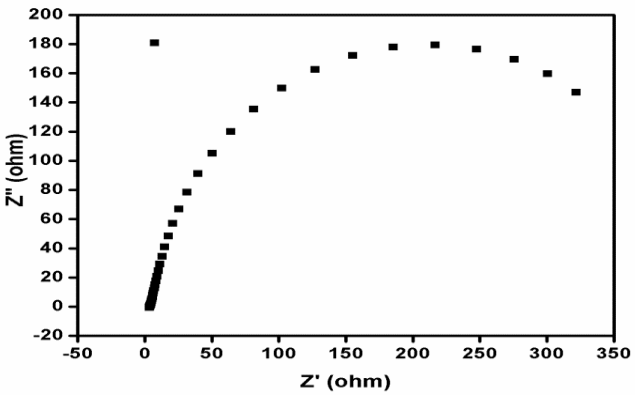

Figure 8: Impedance plot of poly(OMA-co-OCA/ Fe_2O_3 nano composite

Table 3: Electrical Conductivities of (P2ClAn-co-P2OMA/ SDS, (P2ClAn-co-P2OMA)/ Fe_2O_3

Polymers	**Area (Cm^2)**	**Thickness (Cm)**	**Bulk Resistance (S)**	**Conductivity ($S\ cm^{-1}$)**
Poly(OMA-co-OCA)	1	0.005	$4.86x10^{1}$	$2.57x10^{-5}$
Poly(OMA-co-OCA)/ Fe_2O_3	0.25	0.005	$5.46x10^{1}$	$3.36x10^{-4}$

The composite shows higher electrical conductivity than the copolymer and the value is $3.36x\ 10^{-4}$ S cm^{-1} which is in the semiconducting range and can find applications in the field of electronics.

IV. CONCLUSION

Copolymer iron oxide nanocomposite was prepared by in situ polymerization method and is reported by our team for the first time. The FTIR and UV-Vis spectra confirm the formation of polymer iron oxide nanocomposite. The presence of iron oxide nanoparticle in the copolymer influences the electrical conductivity of the nanocomposite. The conductivity studies show that the prepared nanocomposite exhibits semiconducting behavior. The copolymer composite is also thermally more stable than the copolymer. The formation of the nano composite resulted in better processability, improved thermal stability as well as better conductivity.

REFERENCES

[1]. P. Tartaj, M.D Morales, S. Veintemillas-Verdaguer, T. Gonzalez-Carreno, and C.J. Serna, The preparation of magnetic nanoparticles for applications in biomedicine, Journal of Physics D: Applied Physics, 36(13), 2003, 182-197.

[2]. C. Sun, J.S.H. Lee, and M. Zhang, Magnetic nanoparticles in MR imaging and drug delivery, Adv Drug Deliv Rev, 60(11), 2008, 1252–1265.

[3]. P. Li, D.E. Miser, S. Rabiei, R.T. Yadav, and M.R. Hajaligol, The removal of carbon monoxide by iron oxide nanoparticles Appl Catal, B, 43, 2003,151-162.

[4]. S .Sun, C.B. Murray, D .Weller, L. Folks, and A. Moser, Monodisperse FePt nanoparticles and ferromagnetic FePt nanocrystal superlattices, Science, 287(5460), 2000, 1989-1992.

[5]. R. L.N. Chandrakanthi, M.A. Careem, Preparation and Characterization of CdS and Cu 2S Nanoparticle/ Polyaniline Composite Films, Thin Solid Films, 417, 2002, 51-56.

[6]. P.R. Somani, R. Marimuthu, U.P Mulik, S.R Mulik, S.R Sanikar, and D.P. Amalnerkar, High piezoresistivity and its origin in conducting polyaniline/TiO_2 composites, Synth Met, 106, 1999, 45-52.

[7]. Y. He, Synthesis of polyaniline/nano-CeO_2 composite microspheres via a solid – stabilized emulsion route, J. Mater Chem. Phys, 92(1), 2005, 134-137.

[8]. L. Geng, Y. Zhao, X. Huang, S. Wang, S. Zhang, and J. Wu, Characterization and gas sensitivity study of polyaniline/SnO_2 hybrid material prepared by hydrothermal route, Sensors and Actuators B, 120(2), 2007 ,568–572.

[9]. S. Yu, M. Xi, X. Jin, K. Han, Z. Wang, and H. Zhu, Preparation and photoelectrocatalytic properties of polyaniline-intercalated layered manganese oxide film, J.Catalysis Communications, 11(14), 2010, 1125-1128.

[10]. C.C. Buron, B. Lakard, A.F. Monnin, V. Moutarlier, and S. Lakard, Elaboration and Characterization of polyaniline films electrodeposited on tin oxides, .Synth. Met, 161(19), 2011, 2162-2169.

[11]. B. Adhikari, S. Majumdar, Polymers in sensor applications, Prog. Polym.Sci, 29, 2004, 679-766.

[12]. D.T. McQuade, A.E. Pullen, and T.M. Swager, Conjugated polymer-based chemical sensors, Chem, Rev.,100(7) 2000, 2537-74.

[13]. M. Gerard, A. Chaubey, B.D. Malhotra, Application of conducting polymers to biosensors, Biosensors Bioelectronics, 17(5), 2002, 345-59.

[14]. J. P. Chiang, A. G. MacDiarmid, Polyaniline: Protonic Acid Doping Of the Emeraldine Form to the Metallic Regime, Synth. Met, 13, 1986, 193-205.

[15]. R. Sinha, Outlines of polymer technology (New Delhi: Prentice Hall of India Private Limited, 2002).

[16]. C.Laberty, P. Alphonse, J. J. Demai, C. Sarada, A.Rousset, Synthesis and characterization of non stoichiometric nickel manganese spinels, Materials Research Bulletin ,1997, 249 .

[17]. Y.H. Kim, C. Foster , J. Chiang, and A.J. Heeger, Localized charged excitations in polyaniline: infrared photoexcitation and protonation studies, Synth. Met, 29, 1989, 285-290.